TITLE:

CREATION AND PRELIMINARY CHARACTERIZATION OF PREGNANE X RECEPTOR AND CONSTITUTIVE ANDROSTANE RECEPTOR KNOCKOUT RATS

Authors:

Kevin P Forbes, Evguenia Kouranova, Daniel Tinker, Karen Janowski, Doug Cortner, Aaron McCoy and Xiaoxia Cui

Horizon Discovery Group Company, Saint Louis, MO 63146

DMD Fast Forward. Published on July 17, 2017 as DOI: 10.1124/dmd.117.075788
This article has not been copyedited and formatted. The final version may differ from this version.

RUNNING TITLE:

PXR$^{-/-}$ and CAR$^{-/-}$ knock-out rats

Author for correspondence

Name: Kevin P. Forbes

Address: 2033 Westport Center Dr., Saint Louis, MO 63146

Email: k.forbes@horizondiscovery.com

Phone: 314-400-6609

Text pages #: 25

Table #: 5 supplemental tables

Figures #: 5 main figures, 6 supplemental figures

References #: 43

Word count Abstract: 234

Word count Introduction: 745

Word count Results: 1390

Word count Discussion: 1432

Abstract:

The nuclear receptors pregnane X receptor (PXR) and constitutive androstane receptor (CAR) are closely related transcription factors that regulate the expression of Phase I (Cytochrome P450s), Phase II metabolizing enzymes and transporter genes in response to stimulation from xenobiotics, including prescription drugs. PXR and CAR knockout and humanized mouse models have proven useful. However, the rat being bigger in size, is a preferred model system for studying drug metabolism and pharmacokinetics. Here, we report the creation and preliminary characterization of PXR and CAR knockout rats and PXR/CAR double knockout rats. Whereas the expression of phase I and II enzymes and transporter genes were not upregulated by nuclear receptor-specific agonists PCN and TCPOBOP in the knockout rats, confirming the disruption of respective nuclear receptor(s), our data demonstrate that PXR appears to suppress the basal expression levels of Cyp2b2, Cyp3a23/3a1, Cyp3a2, Cyp3a18 and Ugt2b1 genes, while CAR maintains Cyp2b2 and Ugt2b1 and suppresses Cyp3a9 basal expression levels. In wild type rats, agonist binding of the nuclear receptors relieves the suppression, and target genes are expressed at levels comparable to knockout rats, with or without drug treatment. Overall, our findings are in good agreement with data obtained from human primary hepatocytes, nuclear receptor knock-out cell lines and mouse knock-out models. We believe these models are a useful complement to their mouse counterparts for drug development and as importantly, for functional studies on metabolic pathways involving nuclear receptors.

DMD Fast Forward. Published on July 17, 2017 as DOI: 10.1124/dmd.117.075788
This article has not been copyedited and formatted. The final version may differ from this version.

Introduction:

Biological systems are under constant bombardment of endogenous and foreign chemicals (xenobiotics) and have evolved three types of detoxification mechanisms: modification by Phase I enzymes, conjugation by Phase II enzymes, and transport (Xu *et al.*, 2005). A major family of Phase I enzymes are encoded by the cytochrome P450 genes that either deactivate chemicals for their eventual excretion, or convert them into biologically active forms, primarily in the liver and the intestine. These metabolites can be subjected to further breakdown by Phase II enzymes, such as transferases, for elimination. In the last phase, transporter genes contribute to the uptake or efflux of these chemicals and/or the subsequent metabolites (Dogra *et al.*, 1998; Pavek and Dvorak, 2008).

The expression of all three phases of enzymes are believed to be regulated by transcription factors, called nuclear receptors, which bind specific chemicals (ligands). Upon ligand binding, the subset of nuclear receptors that normally reside in the cytoplasm translocate into the nucleus to modulate the transcription of genes encoding enzymes that metabolize the ligands. The pregnane X receptor (PXR, official gene name NR1I2 in human and Nr1i2 in rodents) and constitutive androstane receptor (CAR, official gene name NR1I3 in human and Nr1i3 in rodents) are two vitamin D receptor-like nuclear receptors that belong to the nuclear receptor subfamily 1 (type II). PXR and CAR both have the canonical structure of nuclear receptors, with an N-terminus DNA binding domain (DBD), followed by a hinge and ligand binding domain. At the C-terminus, there is an AF2 (activation function 2) domain that is critical to transcription activation. Each DBD contains two zinc fingers that are conserved across species and between PXR and CAR (Xia and Kemper, 2007; Lichti-Kaiser *et al.*, 2009). Upon ligand binding, both PXR and CAR form a complex with the retinoid X receptor (RXR) at the ligand binding domain as a heterotetramer (PXR-RXR) or

heterodimer (CAR-RXR) (Xu *et al.*, 2004; Wallace *et al.*, 2013). Conformation of the AF2 domain is also changed upon ligand binding and recruits transcriptional activators to turn on target genes. Unlike the AF2 domain of PXR, the AF2 domain of CAR, as its name indicates, once in the nucleus, is constantly active and can turn on transcription without direct ligand binding of CAR (Xu *et al.*, 2004).

Both PXR and CAR are highly conserved receptors across species and in the P450 genes they activate (Mangelsdorf and Evans, 1995; Giguere, 1999; Dickins, 2004; Pelkonen *et al.*, 2008). PXR has primarily been linked to CYP3A (Human CYP3A4; Mouse Cyp3a11) induction and CAR to CYP2B (Human CYP2B6; Mouse Cyp2b10) control. Several other receptors are involved in P450 regulation and there can be significant crosstalk between receptors in terms of their regulation of these genes (Maglich *et al.*, 2002; Dickins, 2004; Wang *et al.*, 2012). In addition, studies have also linked transcriptional regulation of Phase II metabolizing enzymes as well as transporter genes via PXR and CAR (Tolson and Wang, 2010; Aleksunes and Klaassen, 2012; Amacher, 2016)

PXR and CAR can be activated by a variety of species-specific compounds (Timsit and Negishi, 2007; Wang *et al.*, 2012). For example, pregnenlone-16α-carbonitrile (PCN) is a potent ligand for rodent PXR but not for human PXR which has a higher preference for rifampicin (RIF) (Guzelian *et al.*, 2007; Scheer *et al.*, 2008; Slatter *et al.*, 2009). The human CAR is strongly activated by 6-(4-chlorophenyl) imidazo-[2,1-b][1,3] thiazole-5-carbaldehyde O-(3,4-dichloro-benzyl) oxime (CITCO), but the rodent CAR receptor has a preference for 1,4-Bis-[2-(3,5-dichloropyridyloxy)] benzene, 3,3′,5,5′-tetrachloro-1,4-bis(pyridyloxy) benzene (TCPOBOP) not CITCO (Scheer *et al.*, 2008; Slatter *et al.*, 2009). Another compound, phenobarbital (PB), for example, activated both

human and rodent PXR and CAR receptors, as evident by comparing PB treatment of wild-type, knock-out and humanized mouse models (Scheer *et al.*, 2008).

For studies on drug metabolism and pharmacokinetics, compared to mice, the larger size of the rat offers greater blood volume for sampling and higher accuracy in drug dosing. The rat also more closely resembles humans physiologically and allows easier transition into other assays, such as carcinogenicity testing. However, the rat has been under used as a model system due to the historical difficulty of its genome manipulation until the recent availability of nuclease technologies (For review, see the special collection starting with Aitman *et al.*, 2016)

Here, we generated PXR and CAR individual and double knockout rats and characterized the models primarily by observing the effects on Phase I and Phase II drug/xenobiotic metabolizing enzymes and transporter gene expression in the liver with and without drug stimulation.

Materials and Methods:

Zinc-Finger Nucleases (ZFNs). ZFNs to target rat PXR and CAR were obtained from Sigma-Aldrich CompoZR product line. Each ZFN was designed to target within exon 2. ZFN mRNA was in vitro transcribed and validated as described previously (Cui *et al.*, 2011).

Animal husbandry and microinjection. Rat work in this study was performed at SAGE Labs, now part of Horizon Discovery Group Company, which operated under approved animal protocols overseen by SAGE's Institutional Animal Care and Use Committee (IACUC).

Sprague Dawley rats purchased from Charles River Laboratory (USA) were housed in standard cages and maintained on a 12 h light/dark cycle with *ad libitum* access to food and water. Four to five weeks old donors were injected with 20 units of PMS (pregnant mare serum) followed by 50 units of hCG (human chorionic gonadotropin) injection after 48 h and again before mating.

DMD Fast Forward. Published on July 17, 2017 as DOI: 10.1124/dmd.117.075788
This article has not been copyedited and formatted. The final version may differ from this version.

Fertilized eggs were harvested a day later for injection. ZFN mRNA was injected into the pronucleus of fertilized eggs. The final concentration of ZFN mRNA was 10 ng/μL. Recipient female rats were injected with 40 μg of LH-Rh 72 h before mating. Microinjected eggs were transferred to these pseudo-pregnant Sprague Dawley recipients.

Founder Identification and breeding: Live births from microinjections were sampled by toe clipping between 7-21 days after birth. Genomic DNA was purified, screened by PCR with oligonucleotide primers designed to flank the ZFN target site and the PCR products sequenced to verify mutations generated by ZFNS. Methods were described previously (Brown *et al.*, 2013). The following oligonucleotide primers were used for PCR reactions and sequencing: PXR: 5′-TCTTGGAAGAGCCTATCAACG-3′ and 5′-TCCCTTACATCCTTCACAGGTC-3′; CAR: 5′-ACTCCTCCCACATTCAGGAGA-3′ and 5′-GTCTCCACACACCACACAGT-3′. DNA sequencing of PCR products was performed by Elim Biopharma, Inc. (Hayward, CA USA). Founders with desired mutations were bred back to wild-type animals and then intercrossed for breeding to homozygosity and establishing colonies.

Reagents. A mouse monoclonal antibody was generated against a recombinant N-terminal rat PXR protein (Peptide sequence in Supplemental Figure 4) by ProMab Biotechnologies (Richmond, CA USA). PCN and TCPOBOP were obtained from Sigma-Aldrich (St. Louis, MO USA). The chemical structure for PCN found within Kliewer *et al* (1998) and Kelley *et al* (1985) for TCPOBOP.

Drug response test. Eight week old male wild-type, $PXR^{-/-}$, $CAR^{-/-}$ and $PXR^{-/-}/CAR^{-/-}$ rats were treated either with 2.5 mL/kg of corn oil (vehicle), PCN in corn oil (40 mg/mL; Dose equals 100 mg/kg) or TCPOBOP in corn oil (5 mg/mL; Dose equals 12.5 mg/kg) via intraperitoneal (I.P.) injection. PCN and TCPOBOP treatment ranges vary in the literature, the ranges are 20-100 mg/kg

DMD Fast Forward. Published on July 17, 2017 as DOI: 10.1124/dmd.117.075788
This article has not been copyedited and formatted. The final version may differ from this version.

and 1-30 mg/kg respectively. Sixteen hours after injection, rats were euthanized and liver tissues were collected for RNA purification: WT vehicle (n=9), WT PCN and TCPOBOP (n=6); $PXR^{-/-}$ and $CAR^{-/-}$ vehicle, PCN and TCPOBOP (n=3). $PXR^{-/-}/CAR^{-/-}$ vehicle (n=6), PCN and TCPOBOP (n=3).

qRT-PCR. Liver samples were homogenized in TRIzol Reagent (Life Technologies, USA) with ceramic beads using a Precellys homogenizer (PeqLab, Germany.). Total RNA was isolated from homogenate and 100 µg of total RNA was DNAse-I treated and purified (RNA Clean-up) using an RNeasy Mini-kit (Qiagen, USA). First strand cDNA was synthesized from 1µg of purified RNA using the RT^2 First Strand Kit from RT^2 Profiler PCR Array System (Qiagen). First strand cDNA was used in a customized RT^2 Profiler^{TM} PCR Array (Gene list in Supplemental Table 1). All quantitative PCR reactions were performed following the manufacturer's recommended conditions on Bio-Rad's CFX96 Real-Time PCR Detection System. For data analysis of the RT^2 Profiler^{TM} PCR Array, the Ct cutoff was set at 35 (limit of detection) and the average ΔCt was calculated with normalizing to five reference genes (Rplp1, Hprt1, Rpl13a, Ldha, ActB) for each biological replicate.

Taqman assays (Supplemental Table 2; ThermoFisher, USA) for Phase II enzymes and transporters were performed as single-plex reactions following the manufacturer's recommended conditions on Bio-Rad's CFX96 Real-Time PCR Detection System. Biological cDNAs were pooled and assayed in triplicate. Average fold-change was calculated normalizing to three reference genes (ActB, Hprt1 and Gapdh).

For rat PXR and CAR cDNAs, synthesis was performed as above with replacing the kit's random primers with $Oligo(dT)_{20}$ Primer (ThermoFisher, USA), followed by PCR amplification with the following specific oligonucleotides PXR 5′-ATGAGACCTGAGGAGAGG-3′ and 5′-

TCAGCCGTCCGTGCTGCT-3′; CAR 5′-ATGACAGCTACTCTAACA-3′ and 5′-CCGACTTTGGAGTCTTGACTG-3′. PCR amplified cDNAs were resolved by 2% agarose E-Gels (ThermoFisher, USA) for verification of full-length cDNA synthesis and then TA-cloned into pCR4-TOPO (ThermoFisher, USA). DNA sequencing of cloned cDNAs was performed using T7 and T3 primers by Elim Biopharma, Inc. (Hayward, CA USA). Sequence results aligned together using ContigExpress within Vector NTI Advance (Version 11.5.2; ThermoFisher, USA).

Western Blot. Briefly, 100 mg of liver tissue from wild-type and PXR$^{-/-}$ male rats was Dounce homogenized in RIPA buffer plus protease inhibitors. After incubating on ice, the extract was centrifuged to remove debris. The resulting supernatant was resolved by gradient protein gels, transferred to nitrocellulose and then probed with the anti-PXR antibody at 1:500 at room temperature for 1 hour. Secondary anti-mouse heavy plus light chain (Jackson Immuno Research Laboratories, West Grove, PA USA) was used at 1:50,000, room temperature for 1 hour. The blot was developed with Super Signal West Pico (ThermoFisher, USA).

Results:

Generation of PXR and CAR Knockout Rats.

The rat PXR and CAR genes both contain 9 coding exons. Active ZFNs were validated to target exon 2, the first coding exon of both genes coincidently (Figure 1). mRNAs of each pair of ZFNs were combined at 1:1 ratio and microinjected into the pronucleus of fertilized eggs of Sprague Dawley rats, which were then implanted into pseudopregnant females. One of ten live births from PXR ZFN injections carried a 20 base pair (bp) deletion and was bred to establish a homozygous colony. Four of twelve CAR rats had modified alleles, three of which were determined by sequencing to have either a 10 bp or a 12 bp deletion. A male founder with a 10 bp deletion was

used to establish a homozygous colony. A simple PCR at the target site is used as a convenient genotyping screen to differentiate between wild type (WT), heterozygotes and homozygotes alleles (Supplemental Figure 1). Both deletions in PXR and CAR (Supplemental Figure 2A), led to a frameshift in the coding sequence that resulted in pre-mature termination of protein translation in the DNA binding domain (Supplemental Figure 2B). Animals homozygous for the respective deletions are referred to as $PXR^{-/-}$ and $CAR^{-/-}$ rats, and their crossbreeds, $PXR^{-/-}/CAR^{-/-}$ rats.

Confirmation of PXR and CAR gene disruption.

To find out whether the frameshift deletions in $PXR^{-/-}$ and $CAR^{-/-}$ rats led to mRNA degradation via the nonsense mediated decay pathway, we performed quantitative RT-PCR on RNA extracted from liver tissue. Comparable levels of PXR and CAR mRNAs were detected in their respective knockout models as compared to WT rats (data not shown). The deletions did not result in PXR or CAR mRNA degradation via nonsense mediated decay pathway. However, we were able to demonstrate that both mRNAs contain deletions that lead to out-of-frame translation of the messages and nonfunctional proteins (Supplemental Figure 3; Sequence verification of cloned cDNAs amplified with PXR or CAR specific oligonucleotides from WT, $PXR^{-/-}$ and $CAR^{-/-}$ liver RNA).

We then performed Western Blots using a monoclonal antibody raised specifically against the N-terminus of the rat PXR protein (Supplemental Figure 4A-B) on liver protein extracts. Here, we demonstrated that the major PXR peptide was detected in WT rats but absent in $PXR^{-/-}$ samples (Figure 1C), indicating PXR gene disruption by the ZFN-introduced frame-shift. We were unable to find a suitable specific antibody to detect the rat CAR protein in liver extracts.

DMD Fast Forward. Published on July 17, 2017 as DOI: 10.1124/dmd.117.075788
This article has not been copyedited and formatted. The final version may differ from this version.

Impact on body weight by disruption of the nuclear receptors. Male and female WT, $PXR^{-/-}$, $CAR^{-/-}$ and $PXR^{-/-}/CAR^{-/-}$ rats were weighed weekly between the ages of three to fifteen weeks. Over the twelve-week period, male $CAR^{-/-}$ and $PXR^{-/-}/CAR^{-/-}$ rats were both significantly lighter than wild-type rats (t-test; p-value <0.02). However, male $PXR^{-/-}$ rats were heavier than the wild type rats, although not statistically significant (Figure 2A). Female $PXR^{-/-}$ rats were heavier and $CAR^{-/-}$ rats lighter than wild-type rats (t-test; p-value <0.02; Figure 2B) and $PXR^{-/-}/CAR^{-/-}$ rats were indistinguishable from wild type rats (Figure 2B). However, we have to point out that these wild type and knockout rats were not measured within the same time period or same season of the year, which may cause some variability. We superimposed our weight curves onto the wild type rat weight curves available from the vendor webpage, and all the weights fell within the range of 2 standard deviations from the mean (Supplemental Figure 5). We need to be cautious with our conclusions on relative weight change, but believe the general trend is reliable.

Regulation of hepatic Cytochrome P450 genes (Phase I enzymes) in WT, $PXR^{-/-}$ and $CAR^{-/-}$ male rats

We treated male wild-type (WT), $PXR^{-/-}$, $CAR^{-/-}$ and $PXR^{-/-}/CAR^{-/-}$ rats with corn oil (vehicle), PCN (PXR agonist) or TCPOBOP (CAR agonist) in corn oil, collected livers and analyzed gene expression on a custom quantitative RT-PCR array. The array included cytochrome P450 genes, drug transporters, nuclear receptors and controls (Supplemental Table 1). For easier comparison, the relative expression level of each gene is normalized to that of vehicle-treated wild type rats so that both basal expression level changes and drug treatment-mediated expression regulation can be captured in the same graph.

The prototypical cytochrome P450 genes regulated by PXR and CAR, Cyp2b and the Cyp3a subfamily members were analyzed in Figure 3 and Supplemental Table 3. Vehicle-treated samples

are shown in the left clusters of each panel in Figure 3. Cyp2b2 expression was more than 7-fold higher than that of WT in both PXR$^{-/-}$ and PXR$^{-/-}$/CAR$^{-/-}$ rats, whereas in CAR$^{-/-}$ rats, Cyp2b2 mRNA was reduced to about 1/10th of the WT level (Figure 3A). Cyp3a1/3a23, Cyp3a18 and Cyp3a2 expression was also elevated significantly in PXR$^{-/-}$ and PXR$^{-/-}$/CAR$^{-/-}$ rats when compared to WT rats (Figure 3B-D;). However, these genes were not affected by CAR disruption alone (CAR$^{-/-}$, Fig. 3B-D). On the other hand, expression levels of another Cyp3a family member, Cyp3a9, was increased compared to WT levels in CAR$^{-/-}$ and PXR$^{-/-}$/CAR$^{-/-}$ rats but not affected in PXR$^{-/-}$ (Figure 3E). Supplemental Table 3 is a detailed statistical analysis of basal expression levels for these five genes. In the meantime, no significant change in the basal expression level of the other genes within the array, including Cyp1a2, Abcb1a (Mdr1a), Abcb4 (Mdr2), Abcc1 (Mrp1), Abcc2 (Mrp2) and Abcc3 (Mrp3) as an example, was observed (Left cluster; Supplemental Figure 6).

The chemical activation of the rat Cyp2b2 and Cyp3a subfamily members Cyp3a23/3a1, Cyp3a18, Cyp3a2 upon the administration of PCN over vehicle treatment was observed in WT rats and CAR$^{-/-}$ rats, as expected for a PXR agonist (Middle clusters in Figure 3A-E; Table 1). The increased induction of Cyp2b2 by PCN observed in the CAR$^{-/-}$ rats compared to WT rats reflects the activation by PXR upon PCN treatment which compensates for the reduced CAR-dependent basal expression (Figure 3A). Interestingly, Cyp3a9 expression was activated by PCN in WT and PXR$^{-/-}$ and with no significant change in CAR$^{-/-}$ rats (Middle clusters in Figure 3E; Table 1). At the same time, expression levels of Cyp1a2, Abcb1a, Abcb4, Abcc1, Abcc2 and Abcc3 (other genes within the array; data not shown), were unchanged upon PCN treatment in all models (Middle cluster; Supplemental Figure 6).

DMD Fast Forward. Published on July 17, 2017 as DOI: 10.1124/dmd.117.075788
This article has not been copyedited and formatted. The final version may differ from this version.

Treatment with the known CAR agonist TCPOBOP activated Cyp2b2 in WT and PXR$^{-/-}$ rats only, confirming its specificity for a functional CAR gene. Cyp3a23/3a1, Cyp3a18, Cyp3a2 and Cyp3a9 (right clusters in Figure 3 A-E and Table 2), along with Cyp1a2, Abcb1a, Abcb4, Abcc1, Abcc2 and Abcc3 (other genes within the array; data not shown), were not affected by TCPOBOP treatment in any of the models (Right cluster; Supplemental Figure 6).

Regulation of hepatic transporters and Phase II enzymes in WT, PXR$^{-/-}$ and CAR$^{-/-}$ male rats

Solute carrier (Slc) transporters Slco1a1 (Oatp1), Slco1a2 (Oatp2) Slc47a1 (Mate1) and Slc10a1 (Ntcp) were not assayed on the array. We screened RNAs from WT, PXR$^{-/-}$, CAR$^{-/-}$ and PXR$^{-/-}$/CAR$^{-/-}$ rats for changes in basal and activated (PCN and TCPOBOP treatment) expression levels for these transporters separately (Figure 4; statistical analysis Supplemental Table 3 and Table 1 and 2; Taqman assays, Supplemental Table 2). Oatp2 was activated 3- to 4-fold by PCN treatment in WT and CAR$^{-/-}$ rats and unchanged in PXR$^{-/-}$ and PXR$^{-/-}$/CAR$^{-/-}$ (Middle cluster; Figure 4A). There were no observed changes to Oatp1 and Ntcp transporter mRNA levels (Figure 4 B, C) and Mate1 was undetected in our assay (data not shown). In addition, no significant changes were observed in basal expression level or by TCPOBOP treatment in WT or any of the KO models (Left and Right clusters, Figure 4A-C, Table 2).

Phase II enzymes UDP-glucuronosyltransferase (Ugt1a6, Ugt2b1 and Ugt2b7), sulfotransferase (Sult2a2), Glutathione transferase (Gstm4) and Ephx1 basal and activated mRNA levels were determined using the same methods. Basal expression levels of Ugt2b1 was trending down 2-fold in CAR$^{-/-}$and upregulated ~4-fold in PXR$^{-/-}$ and PXR$^{-/-}$/CAR$^{-/-}$ rats and no observed changes in Ugt1a6 when compared to WT (Left clusters; Figure 5A and B; Supplemental Table 3). No significant changes were observed during PCN or TCPOBOP activation (Middle and right clusters; Figure 5A and B) and Ugt2b7 was undetected in our assay (data not shown). Sult2a2 was activated

~5- to 6-fold by PCN treatment in WT and $CAR^{-/-}$ rats and unchanged in $PXR^{-/-}$ and $PXR^{-/-}/CAR^{-/-}$ (Middle cluster; Figure 5C and Table 1). Ephx1was slightly induced by TCPOBOP in $PXR^{-/-}$ and $PXR^{-/-}/CAR^{-/-}$ (Right cluster, Figure 5D) and we observed no changes in Gstm4 mRNA levels (Figure 5E).

Discussion:

In this study, we generated and characterized new knockout rat models for the nuclear receptors PXR and CAR. We observed changes in body weight, basal gene expression levels and loss of receptor mediated activation via exogenous ligands within these knockout lines.

Body weight change in the knockout models confirms the involvement of the nuclear receptors in metabolic pathways other than xenobiotic detoxification. In both genders, disruption of PXR led to weight gain, although in male rats the increase was not statistically significant. In addition, the male double KO rats were significantly lighter than wild type, whereas female double KO rats were comparable to wild type counterparts. The overall trend in rats is that disruption of PXR and CAR had an opposite effect on weight. This suggests that these nuclear receptors function on regulating basal expression levels of opposing sets of genes contributing to body mass. Their effect canceled each other out in the female rats. Similar observations on gender differences were made in mice (Uppal *et al.*, 2005; Anakk *et al.*, 2007), raising the question of whether it is sufficient to only use males for pharmacological tests as the standard method currently. Regardless, weight change is the first indication that the function of these genes were in fact altered in the knockout animals.

As expected, we observed upregulation of Cyp2b2, Cyp3a23/3a1, 3a18, 3a2, 3a9, Slco1a2 (Oatp2) and Sult2a2 genes by PCN compared to by vehicle in WT rats, but not in $PXR^{-/-}$ (Cyp3a9 the

exception; see below about CAR dependent PCN activation) and PXR$^{-/-}$/CAR$^{-/-}$ rats, and upregulation of Cyp2b2 by TCPOBOP in WT and PXR$^{-/-}$ rats, but not in CAR$^{-/-}$ and PXR$^{-/-}$/CAR$^{-/-}$ rats. It is well documented that PCN and TCPOBOP activation of these P450 genes is PXR and CAR-dependent in rodents respectively. The induction of the Oatp2 transporter by PCN has previously been reported in mice (Staudinger *et al.*, 2003; Slatter *et al.*, 2009) and rats (Guo *et al.*, 2002; Slatter *et al.*, 2009) and sulfotransferase (Sult) gene activation in primary rat and human hepatocytes (Fang *et al.*, 2005) and mice (Aleksunes and Klaassen, 2012; Cui and Klaassen, 2016) is PXR dependent. This confirms that hepatic regulation of these genes in rats by PCN is PXR-dependent. We also observed a slight induction of Ephx1 under TCPOBOP activation in PXR$^{-/-}$ (Right cluster, Figure 5D) when compared to WT vehicle treated rats. However, this was not significant when comparing to vehicle treated PXR$^{-/-}$ rats, more than likely due to the slight increase in endogenous Ephx1 levels in these models.

Basal gene expression levels of Cyp2b2, Cyp3a23/3a1, 3a18, 3a2, and Ugt2b1 were increased in PXR$^{-/-}$ rats. Xie et al (2000) first reported on a PXR-null mouse and observed no changes in Cyp3a11 expression levels. However, subsequent studies around PXR in both mice and humans reported changes in genes closely related to the rat counterparts assessed in the current study. In PXR-null mice, Cyp3a11, Oatp2 and Mrp3 had higher basal mRNA levels in the liver than in wild type mice (Staudinger et al., 2001; Staudinger et al., 2003). In humans, allelic variants of PXR genes found in Caucasians and African Americans exhibit altered basal and/or induced transactivation of the CYP3A4 gene (Hustert *et al.*, 2001; Zhang *et al.*, 2001). Compared to PXR$^{-/-}$, in CAR$^{-/-}$ rats, endogenous levels of Cyp3a9 was increased and Cyp2b2 and Ugt2b1 were decreased. In HepaRG cells, an in vitro proliferation-competent human hepatocyte line that closely resembles primary hepatocytes, the disruption of CAR led to changes in basal transcription levels

of several drug metabolizing and transporter genes (Li *et al.*, 2016). In CAR knockout mice, Cyp2b13 (the mouse of equivalent of rat Cyp2b21) expression was upregulated, whereas Cyp2b10 (the mouse equivalent of rat Cyp2b2) expression was down-regulated (Hernadez *et al.*, 2010). In addition to changes in P450 levels, some Phase II enzymes and transporter mRNA expression levels were altered gender dependently in the liver and small intestine of PXR and CAR knock-out mice (Cheng and Klaassen, 2006; Aleksunes and Klaassen, 2012). These reported changes in endogenous gene expression levels is comparable to our observations in $PXR^{-/-}$ and $CAR^{-/-}$ rats. Changes caused by PXR or CAR disruption in basal gene expression levels can confound data analysis when only the ratio of vehicle versus treated samples is looked at.

The disruption of PXR greatly increased the expression levels of Cyp2b2 and Ugt2b1, suggesting that PXR suppresses them directly or indirectly in the absence of exogenous ligand, whereas CAR counterbalances PXR in maintaining their endogenous expression, demonstrated by the diminished Cyp2b2 and Ugt2b1 expression in $CAR^{-/-}$ rats (Figures 3A and 5A; Supplemental Table 3). Similarly, Luiser et al (2014) reported the same phenomenon for Cyp2b10 in PXR and CAR double knock-out mice. Unlike our data, the Ugt2b1 gene is down-regulated only in female TCPOBOP treated CAR-null mice and there is no change at the endogenous level or under PCN treatment in males or females (Aleksunes and Klaassen, 2012). Our observation on the regulation of Ugt2b1 at the endogenous level by both receptors in male rats may be species specific.

The major CYP3A metabolizing enzyme and PXR responsive gene in humans is CYP3A4, Cyp3a11 in mice and Cyp3a23/3a1 in rats. The rat Cyp3a9 is conserved across the other CYP3A "minor" subfamily members in mice (82% identity to Cyp3a13; 65% to Cyp3a11; tblastn, data not shown) and humans (76% to CYP3A7; 75% to CYP3A5; 69% to CYP3A43; 65% to CYP3A4; tblastn, data not shown). Mouse Cyp3a13 is induced by PCN and TCPOBOP (Slatter *et al.*, 2009),

DMD Fast Forward. Published on July 17, 2017 as DOI: 10.1124/dmd.117.075788
This article has not been copyedited and formatted. The final version may differ from this version.

TCPOBOP (Cui and Klaassen, 2016), and the human CYP3A7 and CYP3A43 by RIF (PXR activator) not CITCO (CAR activator) (Kandel *et al.*, 2016). In our study, we observed PCN activation of Cyp3a9 in WT and $PXR^{-/-}$ but not in $CAR^{-/-}$ and $PXR^{-/-}/CAR^{-/-}$. The endogenous levels of Cyp3a9 is significantly elevated in $CAR^{-/-}$ and $PXR^{-/-}/CAR^{-/-}$ and slightly reduced in $PXR^{-/-}$ (not statistically significant) which suggests that CAR suppresses endogenous Cyp3a9 levels in the absence of exogenous ligand. Therefore, CAR regulates Cyp3a9 at the endogenous level and in this case, PCN induced expression, even in PXR KO rats. It is likely some other factors (other nuclear receptors per se) that bind PCN may also regulate Cyp3a9. The expression of the human CYP3A7 and CYP3A5 is elevated in CAR knock-out HepaRG cells when compared to WT with no change to CYP3A43 levels (Li *et al.*, 2016). This suggests that some of the minor CYP3A family members are more CAR dependent than PXR, which regulates the major CYP3A family member across several species.

In summary, as expected, no nuclear receptor-specific agonist-mediated induction of Phase I and Phase II drug/xenobiotic metabolizing enzymes and transporter genes were observed in these knockout rats. Our results also suggest that PXR and CAR are involved in regulation of the basal expression level of different yet overlapping sets of drug metabolizing genes. When both PXR and CAR regulate a given gene, their effects are often counteractive, indicative of crosstalk between the two nuclear receptors. The regulation and signaling crosstalk between PXR and CAR has been linked to several other genes via protein-protein interactions (for review see Oladimeji et al., 2016; Pavek, 2016). This suggests we should look beyond PXR and CARs xenobiotic function and broaden our search for genes involved in other pathways that may be potentially disrupted by the loss of these protein-protein interactions.

Isogenic knockout models provide the perfect tool to dissect functions of individual genes, and these models are also useful in determining drug efficacy with or without nuclear receptors and whether inhibiting NRs would increase efficacy. PXR and CAR are both also drug targets themselves (Cheng *et al.*, 2012; Gao and Xie, 2012; Banerjee *et al.*, 2014). A full understanding of all the pathways the nuclear receptors are involved in would be critical for therapeutic success. Whereas our data only looked at a small portion of pathways PXR and CAR regulate: primarily Phase I and Phase II drug/xenobiotic metabolizing enzymes and transporter expression levels, many other targets may be regulated completely differently. Whole genome RNA profiling in different tissues of wild type and knockout animals would be highly informative on all pathways PXR and CAR are involved in and allow one to better predict metabolism of new drugs as well as potentially target PXR and CAR for therapeutics.

In the meantime, our data showed good correlation between the rat and human responses upon nuclear receptor disruption. These models complement the current mouse models. However, the rat has the advantage of size, and therefore ease of use and precision of measurements. Further studies will be needed to determine the advantage of these rat models over their mouse counterpart.

Acknowledgements:

We would like to thank Dr. Joe Warren and Yumei Wu for micro-injection, Lara Reid, Andre Chambers, Lauren Klaskala and Diana Ji for genotyping and Leanne Mushinski for colony management.

Authorship Contributions:

Participated in research design: Forbes, Kouranova, Cui.

Conducted experiments: Forbes, Kouranova, Tinker, Janowski, Cortner, McCoy.

Performed data analysis: Forbes, Cui.

Wrote or contributed to the writing of the manuscript: Forbes, Cui.

References:

Aitman T, Dhillon P, and Geurts AM (2016) A RATional choice for translational research? *Dis Model Mech* **9**:1069–1072.

Aleksunes LM, and Klaassen CD (2012) Coordinated Regulation of Hepatic Phase-I and -II Drug Metabolizing Genes and Transporters Using AhR-, CAR-, PXR-, PPARalpha-, and Nrf2-null Mice. *Drug Metab Dispos* **40**:1366–1379.

Amacher DE (2016) The regulation of human hepatic drug transporter expression by activation of xenobiotic-sensing nuclear receptors. *Expert Opin Drug Metab Toxicol* **12**:1463–1477, England.

Anakk S, Huang W, Staudinger JL, Tan K, Cole TJ, Moore DD, and Strobel HW (2007) Gender dictates the nuclear receptor-mediated regulation of CYP3A44. *Drug Metab Dispos* **35**:36–42.

Banerjee M, Robbins D, and Chen T (2014) Targeting xenobiotic receptors PXR and CAR in human diseases. *Drug Discov Today* **20**:618–628, Elsevier Ltd.

Brown AJ, Fisher DA, Kouranova E, McCoy A, Forbes K, Wu Y, Henry R, Ji D, Chambers A, Warren J, Shu W, Weinstein EJ, and Cui X (2013) Whole-rat conditional gene knockout via genome editing. *Nat Methods* **10**:638–40.

Cheng J, Shah YM, and Gonzalez FJ (2012) Pregnane X receptor as a target for treatment of inflammatory bowel disorders.

Cheng X, and Klaassen CD (2006) Regulation of mRNA expression of xenobiotic transporters by the pregnane x receptor in mouse liver, kidney, and intestine. *Drug Metab Dispos* **34**:1863–7.

Cui JY, and Klaassen CD (2016) RNA-Seq reveals common and unique PXR- and CAR-target gene signatures in the mouse liver transcriptome. *Biochim Biophys Acta - Gene Regul Mech* **1859**:1198–1217, Elsevier B.V.

Cui X, Ji D, Fisher DA, Wu Y, Briner DM, and Weinstein EJ (2011) Targeted integration in rat and mouse embryos with zinc-finger nucleases. *Nat Biotechnol* **29**:64–67.

Dickins M (2004) Induction of cytochromes P450. *Curr Top Med Chem* **4**:1745–1766, Netherlands.

Dogra SC, Whitelaw ML, and May BK (1998) Transcriptional activation of cytochrome P450 genes by different classes of chemical inducers. *Clin Exp Pharmacol Physiol* **25**:1–9.

Fang H, Strom SC, Cai H, Falany CN, Kocarek TA, and Runge-morris M (2005) Regulation of Human Hepatic Hydroxysteroid Sulfotransferase Gene Expression by the Peroxisome Proliferator-Activated Receptor-alpha Transcription Factor. *Mol Pharmacol* **67**:1257–1267.

Gao J, and Xie W (2012) Targeting xenobiotic receptors PXR and CAR for metabolic diseases. *Trends Pharmacol Sci* **33**:552–558.

Giguere V (1999) Orphan nuclear receptors: from gene to function. *Endocr Rev* **20**:689–725, UNITED STATES.

Guo GL, Staudinger J, Ogura K, and Klaassen CD (2002) Induction of Rat Organic Anion Transporting Polypeptide 2 by Pregnenolone-16 ␣ -carbonitrile Is via Interaction with Pregnane X Receptor. **61**:832–839.

Guzelian J, Barwick JL, Hunter L, Phang TL, Linda C, and Guzelian PS (2007) Identification of Genes Controlled by the Pregnane X Receptor by Microarray Analysis of mRNAs from Pregnenolone 16α-carbonitrile Treated Rats. *Toxicol Sci* **94**:379–387.

Hernadez J, Mota L, Huang W, Morre D, and Baldwin W (2010) Sexually dimorphic regulation and induction of P450s by the constitutive androstane receptor (CAR). *Toxicology* **256**:53–64.

Hustert E, Zibat A, Presecan-Siedel E, Eiselt R, Mueller R, Fuss C, Brehm I, Brinkmann U, Eichelbaum M, Wojnowski L, and Burk O (2001) Natural protein variants of pregnane X receptor with altered transactivation activity toward CYP3A4. *Drug Metab Dispos* **29**:1454–1459.

Kandel BA, Thomas M, Winter S, Damm G, Seehofer D, Burk O, Schwab M, and Zanger UM (2016) Genomewide comparison of the inducible transcriptomes of nuclear receptors CAR, PXR and PPARalpha in primary human hepatocytes. *Biochim Biophys Acta - Gene Regul Mech* **1859**:1218–1227, Netherlands.

Kelley M, Lambert I, Merrill J, and Safe S (1985) 1,4-Bis[2-(3,5-dichloropyridyloxy)]benzene (TCPOBOP) and related compounds as inducers of hepatic monooxygenases. Structure-activity effects. *Biochem Pharmacol* **34**:3489–3494, England.

Kliewer SA, Moore JT, Wade L, Staudinger JL, Watson MA, Jones SA, McKee DD, Oliver BB, Willson TM, Zetterström RH, Perlmann T, and Lehmann JM (1998) An orphan nuclear receptor activated by pregnanes defines a novel steroid signaling pathway. *Cell* **92**:73–82.

Li D, Mackowiak B, Brayman TG, Mitchell M, Zhang L, Huang S, Wang H, and Spring S (2016) Genome-wide Analysis of Human Constitutive Androstane Receptor (CAR) Transcriptome in Wild-type and CAR-knockout HepaRG cells. *Biochem Pharmacol* **98**:190–202.

Lichti-Kaiser K, Xu C, and Staudinger JL (2009) Cyclic AMP-dependent protein kinase

signaling modulates pregnane x receptor activity in a species-specific manner. *J Biol Chem* **284**:6639–49.

Luisier R, Lempiainen H, Scherbichler N, Braeuning A, Geissler M, Dubost V, Muller A, Scheer N, Chibout S-D, Hara H, Picard F, Theil D, Couttet P, Vitobello A, Grenet O, Grasl-Kraupp B, Ellinger-Ziegelbauer H, Thomson JP, Meehan RR, Elcombe CR, Henderson CJ, Wolf CR, Schwarz M, Moulin P, Terranova R, and Moggs JG (2014) Phenobarbital Induces Cell Cycle Transcriptional Responses in Mouse Liver Humanized for Constitutive Androstane and Pregnane X Receptors. *Toxicol Sci* **139**:501–511.

Maglich JM, Stoltz CM, Goodwin B, Hawkins-Brown D, Moore JT, and Kliewer SA (2002) Nuclear Pregnane X Receptor and Constitutive Androstane Receptor Regulate Overlapping but Distinct Sets of Genes Involved in Xenobiotic Detoxification. *Mol Pharmacol* **62**:638–646.

Mangelsdorf DJ, and Evans RM (1995) The RXR heterodimers and orphan receptors. *Cell* **83**:841–850.

Oladimeji P, Cui H, Zhang C, and Chen T (2016) Regulation of PXR and CAR by protein-protein interaction and signaling crosstalk. *Expert Opin Drug Metab Toxicol* 1–14.

Pavek P (2016) Pregnane X Receptor (PXR)-Mediated Gene Repression and Cross-Talk of PXR with Other Nuclear Receptors via Coactivator Interactions. *Front Pharmacol* **7**:1–16.

Pavek P, and Dvorak Z (2008) Xenobiotic-induced transcriptional regulation of xenobiotic metabolizing enzymes of the cytochrome P450 superfamily in human extrahepatic tissues. *Curr Drug Metab* **9**:129–143, Netherlands.

Pelkonen O, Turpeinen M, Hakkola J, Honkakoski P, Hukkanen J, and Raunio H (2008)

Inhibition and induction of human cytochrome P450 enzymes: Current status. *Arch Toxicol* **82**:667–715.

Scheer N, Ross J, Rode A, Zevnik B, Niehaves S, Faust N, and Wolf CR (2008) Technical advance A novel panel of mouse models to evaluate the role of human pregnane X receptor and constitutive androstane receptor in drug response. *J Clin Invest* **118**.

Slatter JG, Cheng O, Cornwell PD, de Souza A, Rockett J, Rushmore T, Hartley D, Evers R, He Y, Dai X, Hu R, Caguyong M, Roberts CJ, Castle J, and Ulrich RG (2009) Microarray-based compendium of hepatic gene expression profiles for prototypical ADME gene-inducing compounds in rats and mice in vivo. *Xenobiotica* **36**:902–937.

Staudinger JL, Goodwin B, Jones S a, Hawkins-Brown D, MacKenzie KI, LaTour a, Liu Y, Klaassen CD, Brown KK, Reinhard J, Willson TM, Koller BH, and Kliewer S a (2001) The nuclear receptor PXR is a lithocholic acid sensor that protects against liver toxicity. *Proc Natl Acad Sci U S A* **98**:3369–74.

Staudinger JL, Madan A, Carol KM, and Parkinson A (2003) Regulation of drug transporter gene expression by nuclear receptors. *Drug Metab Dispos* **31**:523–527.

Timsit YE, and Negishi M (2007) CAR and PXR: the xenobiotic-sensing receptors. *Steroids* **72**:231–246, United States.

Tolson AH, and Wang H (2010) Regulation of drug-metabolizing enzymes by xenobiotic receptors: PXR and CAR. *Adv Drug Deliv Rev* **62**:1238–1249, Netherlands.

Uppal H, Toma D, Saini SPS, Ren S, Jones TJ, and Xie W (2005) Combined loss of orphan receptor PXR and CAR heightens sensitivity to toxic bile acids in mice. *Hepatology* **41**:168–176.

Wallace BD, Betts L, Talmage G, Pollet RM, Holman NS, and Redinbo MR (2013) Structural and Functional Analysis of the Human Nuclear Xenobiotic Receptor PXR in Complex with RXRα. *J Mol Biol* **425**:2561–2577.

Wang Y-M, Ong SS, Chai SC, and Chen T (2012) Role of CAR and PXR in xenobiotic sensing and metabolism. *Expert Opin Drug Metab Toxicol* **8**:803–817, England.

Xia J, and Kemper B (2007) Subcellular trafficking signals of constitutive androstane receptor: evidence for a nuclear export signal in the DNA-binding domain. *Drug Metab Dispos* **35**:1489–1494, United States.

Xie W, Barwick JL, Downes M, Blumberg B, Simon CM, Nelson MC, Neuschwander-Tetri BA, Brunt EM, Guzelian PS, and Evans RM (2000) Humanized xenobiotic response in mice expressing nuclear receptor SXR. *Nature* **406**:435–439.

Xu C, Li CY-T, and Kong A-NT (2005) Induction of phase I, II and III drug metabolism/transport by xenobiotics. *Arch Pharm Res* **28**:249–268, Korea (South).

Xu RX, Lambert MH, Wisely BB, Warren EN, Weinert EE, Waitt GM, Williams JD, Collins JL, Moore LB, Willson TM, and Moore JT (2004) A structural basis for constitutive activity in the human CAR/RXRalpha heterodimer. *Mol Cell* **16**:919–928, United States.

Zhang J, Kuehl P, Green ED, Touchman JW, Watkins PB, Daly A, Hall SD, Maurel P, Relling M, Brimer C, Yasuda K, Wrighton SA, Hancock M, Kim RB, Strom S, Thummel K, Russell CG, Hudson JR, Schuetz EG, and Boguski MS (2001) The human pregnane X receptor: genomic structure and identification and functional characterization of natural allelic variants. *Pharmacogenetics* **11**:555–572.

Footnotes:

Competing interests statement:

All of the authors are full-time employees of Horizon Discovery, a CRO that sells the rat models described in the paper as well as provides drug testing services using these models.

DMD Fast Forward. Published on July 17, 2017 as DOI: 10.1124/dmd.117.075788
This article has not been copyedited and formatted. The final version may differ from this version.

Figure Legends:

Figure 1. Deletion map for PXR and CAR Genes Generated via ZFNs. The rat PXR (A) and CAR (B) transcripts each contain 9 exons. Black boxes with numbers represent exons and dashes introns. A double hash mark represents exons not shown (Exons 4 to 8 for both genes). Top sequence is the ZFN target sequence and bottom sequence with dashes represent mutant allele. (C) Wild-type (WT) and $PXR^{-/-}$ liver protein extracts were analyzed for PXR expression by immunoblotting. Actin was used as an internal control. The size of the 50kD protein marker is listed on the left and the corresponding PXR and Actin band on the right of the gel with a solid dash mark.

Figure 2. Weight curves. Male (**A**) and female (**B**) wild-type (WT), $PXR^{-/-}$, $CAR^{-/-}$, and $PXR^{-/-}$ /$CAR^{-/-}$ null animals were weighed (in grams) weekly starting at 3 weeks of age up to 15 weeks. The legend represents the plot order, from top to bottom, for simplicity. The order in A and B is $PXR^{-/-}$, WT, $PXR^{-/-}$/$CAR^{-/-}$- and $CAR^{-/-}$. Error bars represent calculated standard deviation.

Figure 3. Fold Change in P450 Gene Expression Levels in Untreated and Treated WT and Knock-out Rats. Vehicle (*left cluster*), PCN (*middle cluster*) and TCPOBOP (*right cluster*) treated rats Cyp2b2 (A), 3a23/3a1 (B), 3a18 (C), 3a2 (D) and 3a9 (E) expression levels were normalized to WT vehicle treated rats to calculate fold changes. Fold change calculated by dividing each $2^{-\Delta CT}$ replicate (biologic) by the average WT vehicle $2^{-\Delta CT}$. Error bars are calculated standard deviation between the biological replicates. Dashed line represent normalized WT vehicle average value of 1. Asterisk marks (*) represent calculated p-values; two-way ANOVA followed by Tukey's multiple comparison test ($p<0.05$, Tukey's). Bars marked with an asterisk mark (*) are significantly different than WT vehicle treated rats.

Figure 4. Fold Change in Transporter Gene Expression Levels in Untreated and Treated WT and Knock-out Rats. Vehicle (*left cluster*), PCN (*middle cluster*) and TCPOBOP (*right cluster*) treated rats Slco1a2 (A), Slco1a1 (B) and Slc10a1 (C) expression levels were normalized to WT vehicle treated rats to calculate fold changes. Fold change calculated by dividing each $2^{-\Delta CT}$ replicate reaction by the average WT vehicle $2^{-\Delta CT}$. Error bars are calculated standard deviation between replicate reactions. Dashed line represent normalized WT vehicle average value of 1. Asterisk marks (*) represent calculated p-values; two-way ANOVA followed by Tukey's multiple comparison test ($p<0.05$, Tukey's). Bars marked with an asterisk mark (*) are significantly different than WT vehicle treated rats.

Figure 5. Fold Change in Phase II Enzyme Gene Expression Levels in Untreated and Treated WT and Knock-out Rats. Vehicle (*left cluster*), PCN (*middle cluster*) and TCPOBOP (*right cluster*) treated rats Ugt2b1 (A), Ugt1a6 (B), Sult2a2 (C), Ephx1 (D) and Gstm4(E) expression levels were normalized to WT vehicle treated rats to calculate fold changes. Fold change calculated by dividing each $2^{-\Delta CT}$ replicate reaction by the average WT vehicle $2^{-\Delta CT}$. Error bars are calculated standard deviation between the replicate reactions. Dashed line represent normalized WT vehicle average value of 1. A second dash line of a value of 2 added (D) to represent the range of significant change in gene expression. Asterisk marks (*) represent calculated p-values; two-way ANOVA followed by Tukey's multiple comparison test ($p<0.05$, Tukey's). Bars marked with an asterisk mark (*) are significantly different than WT vehicle treated rats.

DMD Fast Forward. Published on July 17, 2017 as DOI: 10.1124/dmd.117.075788
This article has not been copyedited and formatted. The final version may differ from this version.

Table 1. Fold Change of Gene Expression in PCN:Vehicle Treated Rats

P450 Gene	WT	PXR$^{-/-}$	CAR$^{-/-}$	PXR$^{-/-}$/CAR$^{-/-}$
Cyp2b2	2.42*	1.65	26.76	1.09
	(+/- 0.85)	(+/- 0.50)	(+/- 23.56)	(+/- 0.35)
Cyp3a23/3a1	5.30*	1.23**	8.08	1.24**
	(+/- 1.32)	(+/- 0.27)	(+/- 4.60)	(+/- 0.29)
Cyp3a18	3.78*	1.19**	4.86*	1.19**
	(+/- 1.23)	(+/- 0.24)	(+/- 2.22)	(+/- 0.13)
Cyp3a2	2.83*	1.25	2.58*	0.82
	(+/- 2.23)	(+/- 0.36)	(+/- 0.70)	(+/- 0.35)
Cyp3a9	2.89*	4.31*	2.07	1.24
	(+/- 0.84)	(+/- 2.03)	(+/- 1.06)	(+/- 0.33)
Slco1a2	3.30*	1.00**	3.82*	0.93**
	(+/- 1.13)	(+/- 0.20)	(+/- 1.01)	(+/- 0.15)
Slco1a1	1.34	0.81	0.65	0.64
	(+/- 0.55)	(+/- 0.37)	(+/- 0.08)	(+/- 0.13)
Slc10a1	1.06	1.06	0.94	0.85
	(+/- 0.36)	(+/- 0.21)	(+/- 0.25)	(+/- 0.14)
Ugt2b1	1.87	0.68	3.65*/**	0.62
	(+/- 0.62)	(+/- 0.18)	(+/- 0.97)	(+/- 0.17)
Ugt1a6	0.70	0.68	0.79	0.43
	(+/- 0.24)	(+/-0.13)	(+/- 0.21)	(+/- 0.07)
Sult2a2	5.71*	0.67**	5.04*	0.43**
	(+/- 1.91)	(+/- 0.18)	(+/- 1.35)	(+/- 0.12)
Ephx1	1.24	0.80	0.84	0.43
	(+/- 0.42)	(+/- 0.16)	(+/- 0.22)	(+/- 0.07)
Gstm4	0.82	0.70	0.64	0.93
	(+/- 0.28)	(+/- 0.14)	(+/- 0.17)	(+/- 0.15)

Values are fold change PCN to vehicle treated, +/- standard deviation.
* = significantly different from vehicle treated, same genotype ($p<0.05$, t-test). Fold change between genotypes analyzed by one-way ANOVA followed by Tukey's multiple comparison test. ** = significantly different from WT ($p<0.05$, Tukey's)

DMD Fast Forward. Published on July 17, 2017 as DOI: 10.1124/dmd.117.075788
This article has not been copyedited and formatted. The final version may differ from this version.

Table 2. Fold Change of Gene Expression in TCPOBOP:Vehicle Treated Rats

P450 Gene	WT	PXR$^{-/-}$	CAR$^{-/-}$	PXR$^{-/-}$/CAR$^{-/-}$
Cyp2b2	6.18*	3.65*	1.42**	0.71**
	(+/- 2.38)	(+/- 0.83)	(+/- 1.05)	(+/- 0.41)
Cyp3a23/3a1	1.08	1.44	0.99	0.69
	(+/- 0.31)	(+/- 0.08)	(+/- 0.22)	(+/- 0.14)
Cyp3a18	1.06	1.21	1.00	0.76
	(+/- 0.29)	(+/- 0.17)	(+/- 0.23)	(+/- 0.15)
Cyp3a2	1.07	1.38	0.87	0.20
	(+/- 0.23)	(+/- 0.34)	(+/- 0.24)	(+/- 0.03)
Cyp3a9	1.68	5.38	0.70	0.27
	(+/- 0.84)	(+/- 5.35)	(+/- 0.27)	(+/- 0.20)
Slco1a2	1.10	0.88	0.95	1.26
	(+/- 0.17)	(+/- 0.24)	(+/- 0.31)	(+/- 0.28)
Slco1a1	0.82	0.79	0.63	1.19
	(+/- 0.14)	(+/- 0.37)	(+/- 0.11)	(+/- 0.24)
Slc10a1	0.92	1.25	1.15	1.26
	(+/- 0.14)	(+/- 0.35)	(+/- 0.37)	(+/- 0.28)
Ugt2b1	1.04	0.94	0.55	1.45
	(+/- .014)	(+/- 0.09)	(+/- 0.19)	(+/- 0.84)
Ugt1a6	0.78	1.15	1.26	1.21
	(+/- 0.12)	(+/- 0.32)	(+/- 0.41)	(+/- 0.27)
Sult2a2	1.20	0.42*	2.35*	1.16
	(+/- 0.16)	(+/- 0.04)	(+/- 0.80)	(+/- 0.67)
Ephx1	1.34	1.74	0.85	1.54
	(+/- 0.20)	(+/- 0.48)	(+/- 0.28)	(+/- 0.34)
Gstm4	0.65	0.92	0.59	1.26
	(+/- 0.10)	(+/- 0.25)	(+/- 0.19)	(+/- 0.28)

Values are fold change TCPOBOP to vehicle treated, +/- standard deviation.
* = significantly different from vehicle treated, same genotype ($p<0.05$, t-test).
Fold change between genotypes analyzed by one-way ANOVA followed by Tukey's multiple comparison test. ** = significantly different from WT ($p<0.05$, Tukey's)

DMD Fast Forward. Published on July 17, 2017 as DOI: 10.1124/dmd.117.075788
This article has not been copyedited and formatted. The final version may differ from this version.

Figure 1.

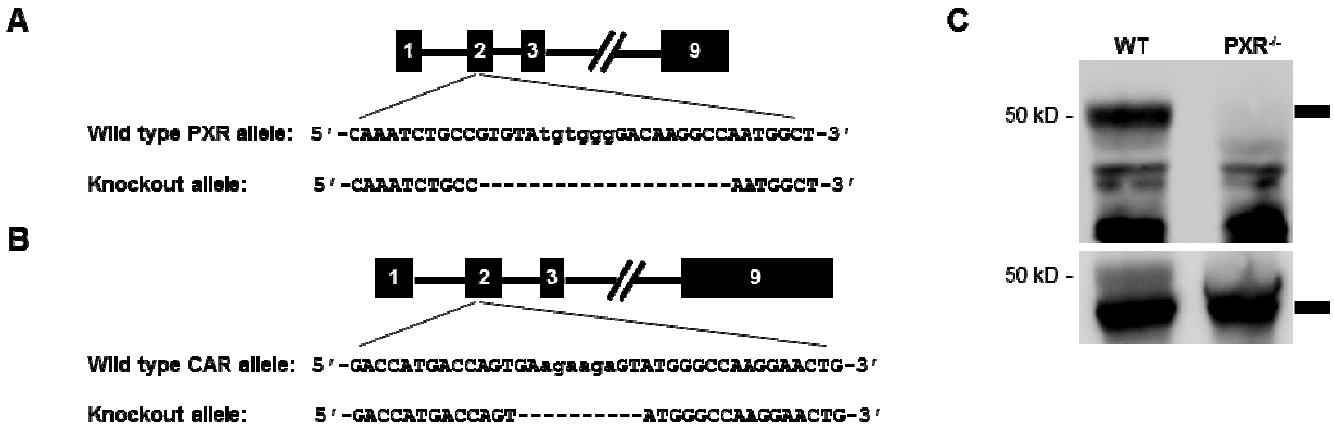

DMD Fast Forward. Published on July 17, 2017 as DOI: 10.1124/dmd.117.075788
This article has not been copyedited and formatted. The final version may differ from this version.

Figure 2.

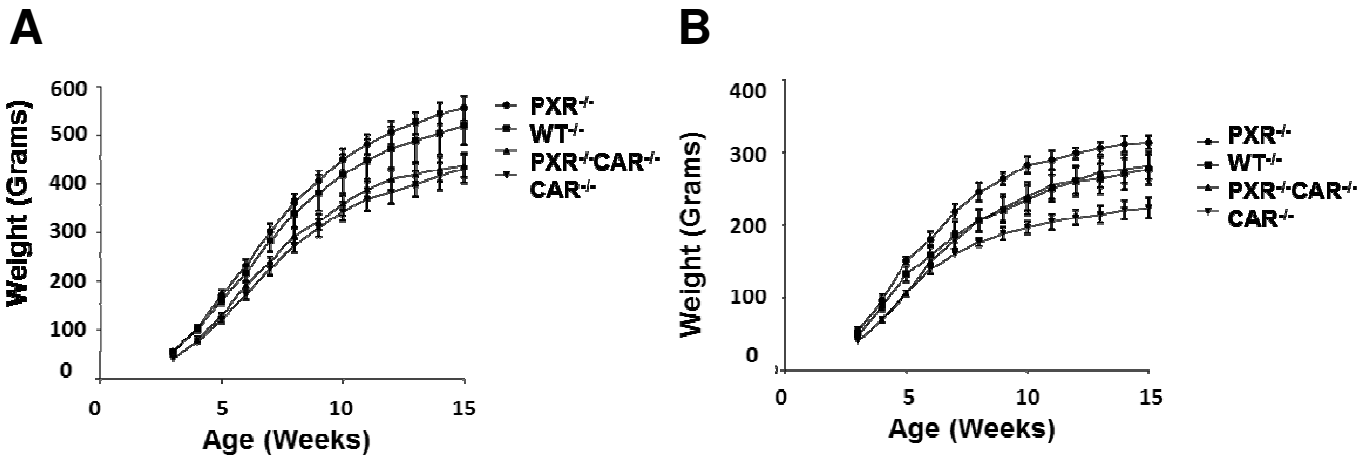

DMD Fast Forward. Published on July 17, 2017 as DOI: 10.1124/dmd.117.075788
This article has not been copyedited and formatted. The final version may differ from this version.

Figure 3.

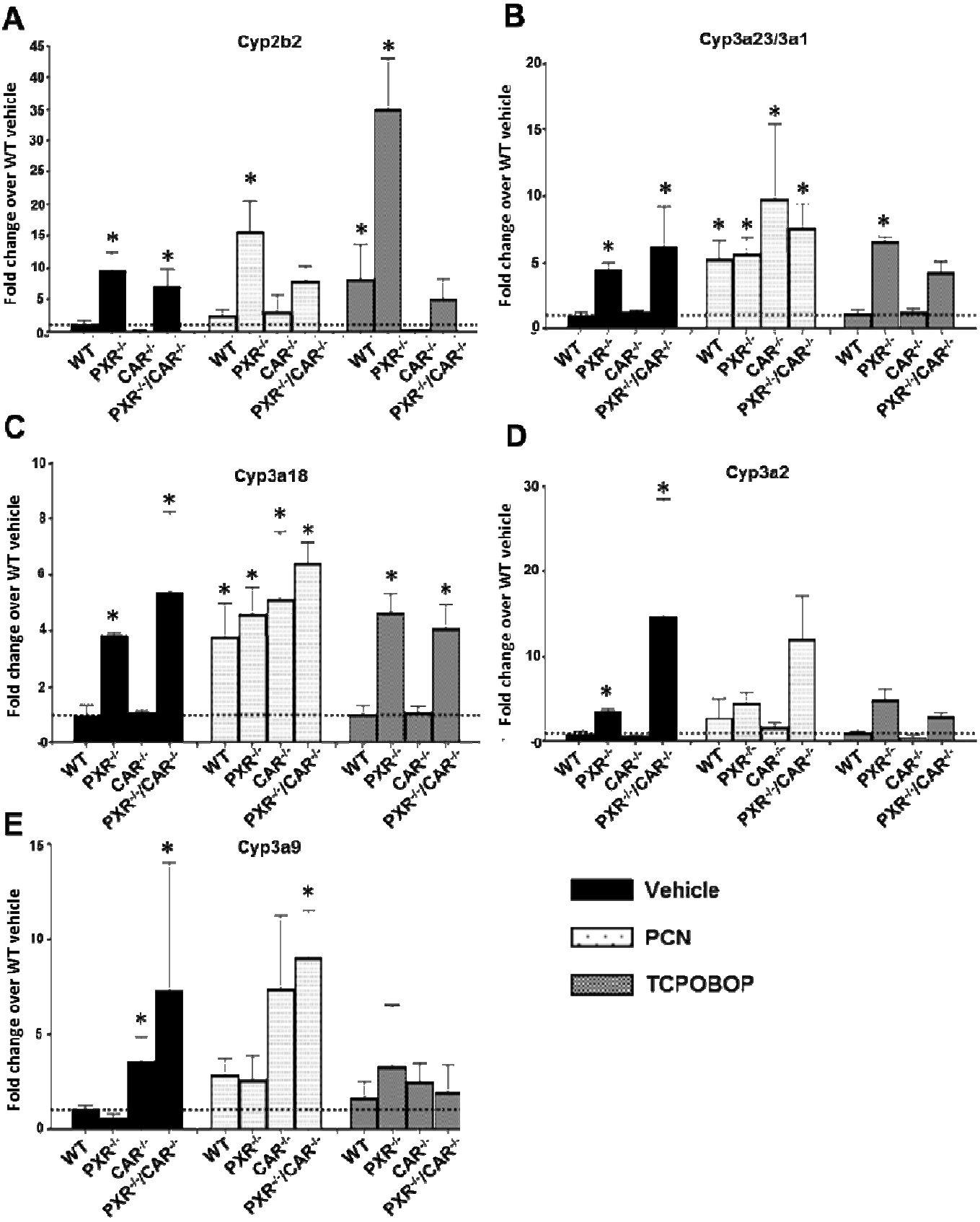

DMD Fast Forward. Published on July 17, 2017 as DOI: 10.1124/dmd.117.075788
This article has not been copyedited and formatted. The final version may differ from this version.

Figure 4.

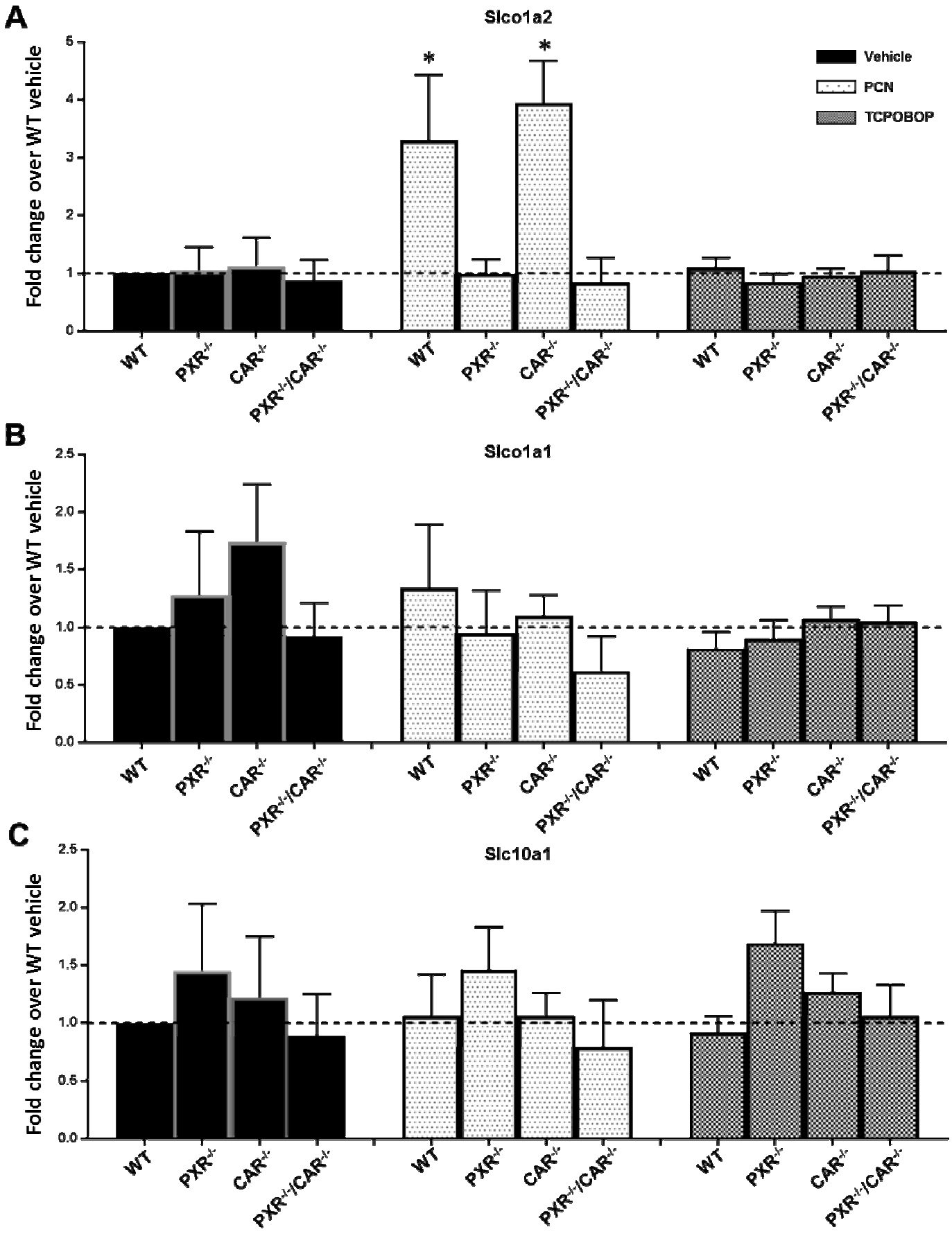

DMD Fast Forward. Published on July 17, 2017 as DOI: 10.1124/dmd.117.075788
This article has not been copyedited and formatted. The final version may differ from this version.

Figure 5.

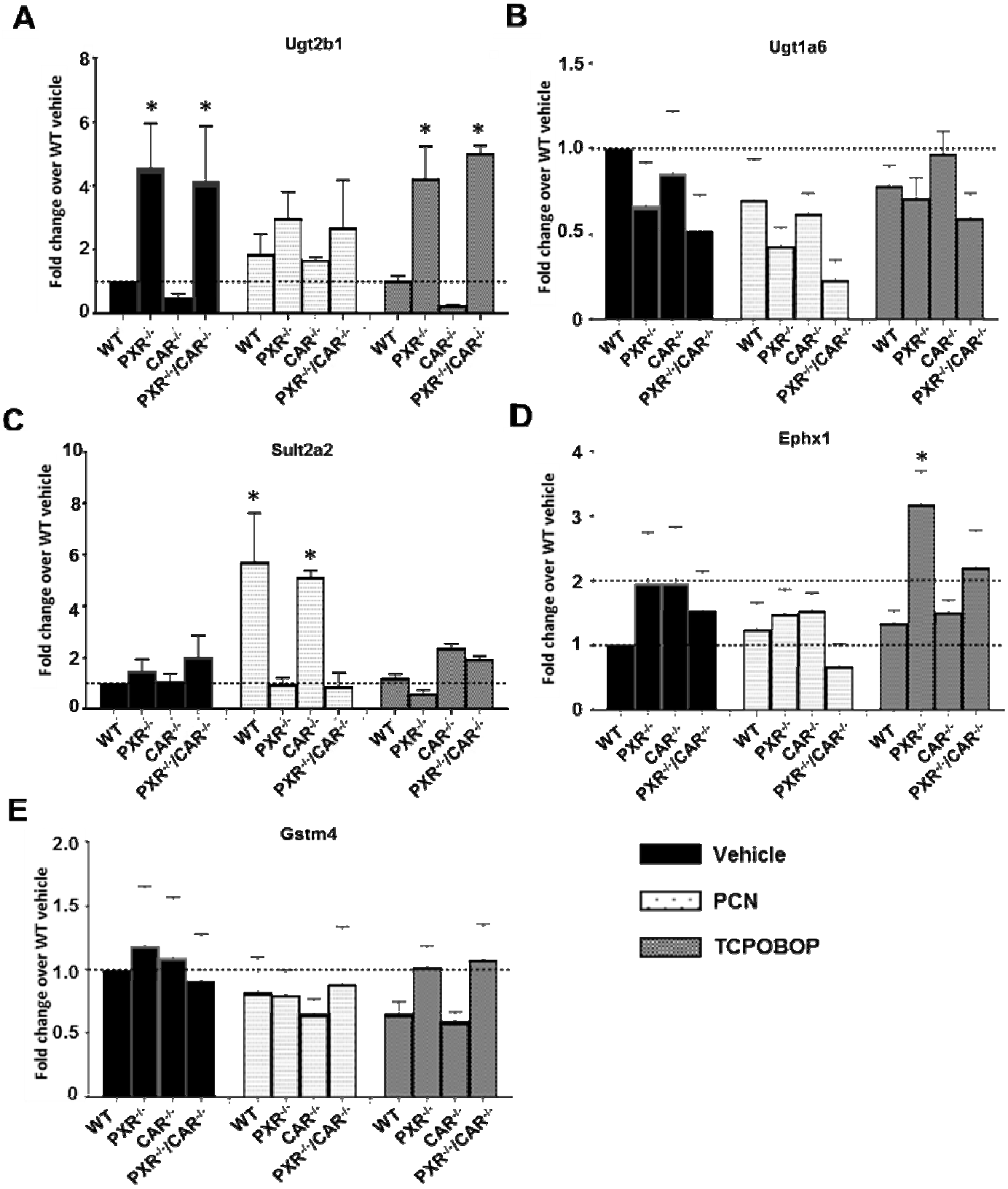

CREATION AND PRELIMINARY CHARACTERIZATION OF PREGNANE X RECEPTOR AND CONSTITUTIVE ANDROSTANE RECEPTOR KNOCKOUT RATS

Kevin P Forbes, Evguenia Kouranova, Daniel Tinker, Karen Janowski, Doug Cortner, Aaron McCoy and Xiaoxia Cui

Drug Metabolism Disposition

Supplemental Figure 1.

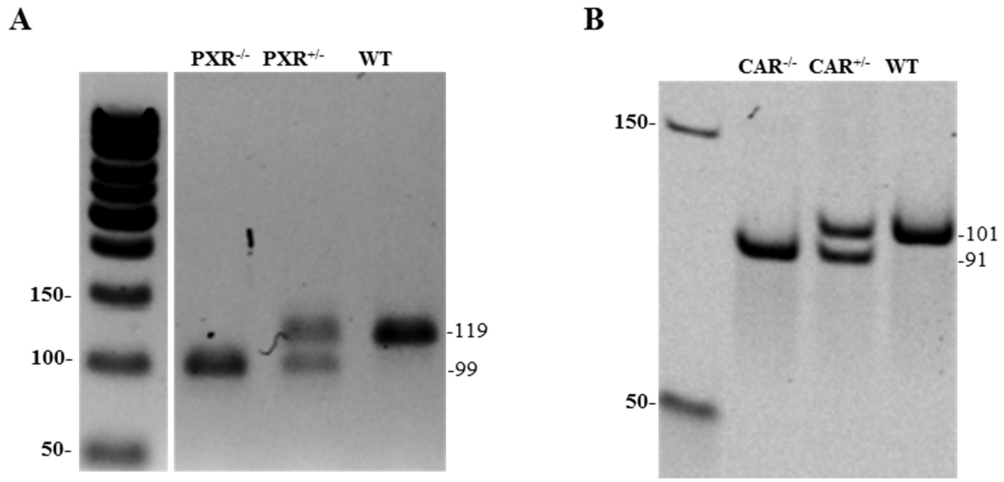

Supplemental Figure 1. PCR Genotyping for PXR$^{-/-}$ and CAR$^{-/-}$. PCR reactions using primers that flank the ZFN target site for PXR (A) and CAR (B) genes were resolved by agarose gels. Reactions corresponding to the WT, het ($^{+/-}$) and hom ($^{-/-}$) for the knock-out of PXR and CAR genes are listed above each gel. Sizes in base pairs (bp) of the WT (119bp, PXR; 101bp, CAR) and mutant alleles (99bp, PXR; 91bp, CAR) are listed on the right of each gel with DNA ladders sizes listed on the left.

Supplemental Figure 2.

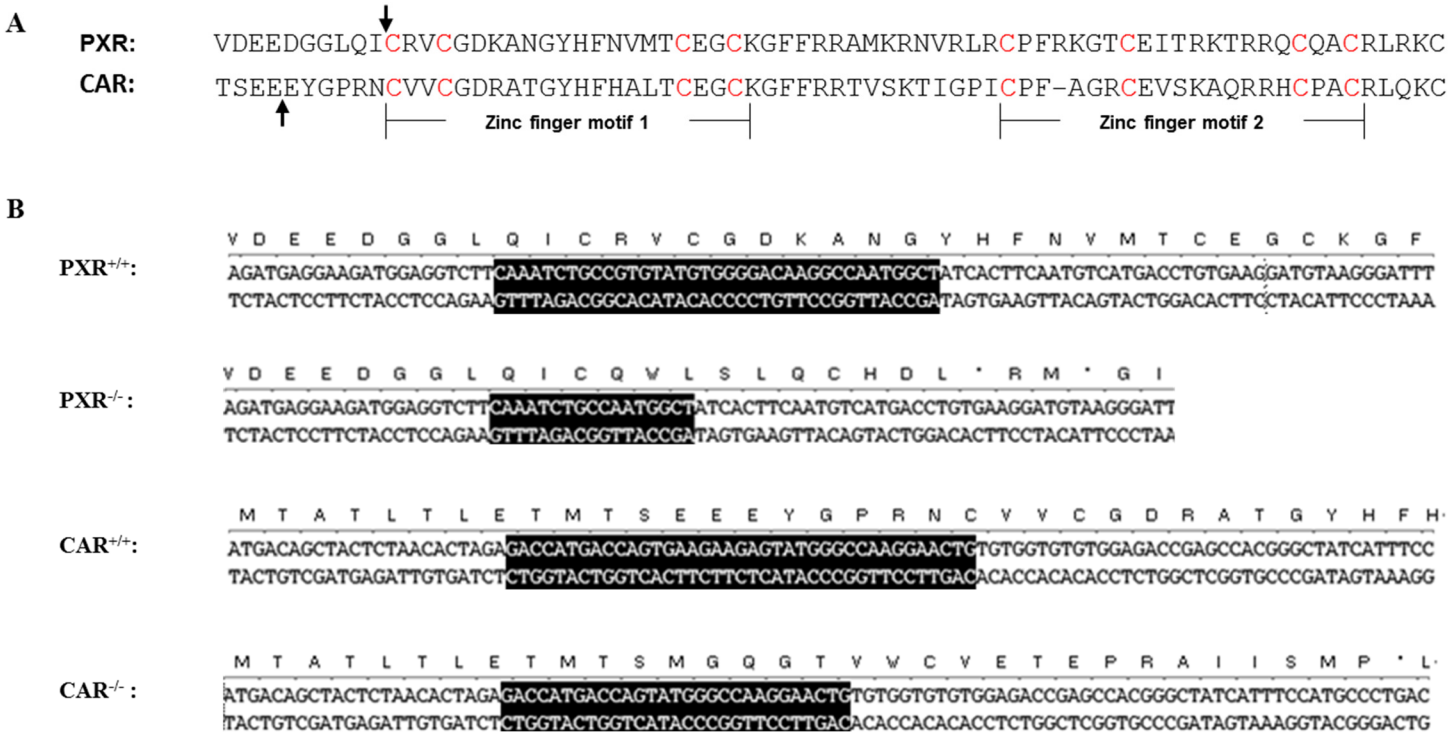

Supplemental Figure 2. Deletions in PXR$^{-/-}$ and CAR$^{-/-}$ rats. A. PXR and CAR protein sequence and structure at the deletion sites. Zinc finger motifs 1 and 2 in the DNA binding domain are highly conserved across species and between CAR and PXR. Each motif contains four cysteines (in red) that bind a Zinc ion. Arrows indicate the beginning of deletions in the knockout alleles, respectively. B. Coding sequences around the ZFN target sites in PXR and CAR genes. In wild type sequences (PXR$^{+/+}$ and CAR$^{+/+}$), ZFN recognition sites are highlighted. In the knockout sequences (PXR$^{-/-}$ and CAR$^{-/-}$), ZFN recognition sites that are left from the deletions are highlighted. Predicted premature stop codons (asterisks) introduced by frameshift.

Supplemental Figure 3.

A

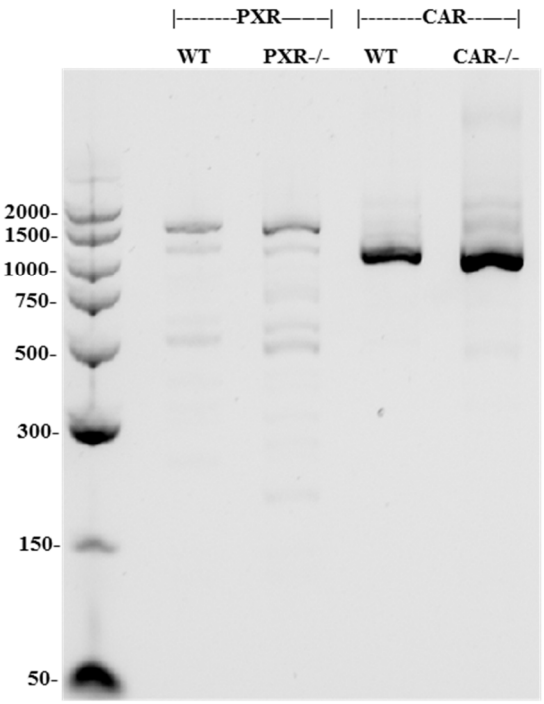

B

```
» PXR KO-1 CGTAGATGAGGAAGATGGAGGTCTTCAAATCTGCC--------------------AATGGCTATCACTTCAATGTCATGAC
» PXR KO-2 CGTAGATGAGGAAGATGGAGGTCTTCAAATCTGCC--------------------AATGGCTATCACTTCAATGTCATGAC
» PXR KO-3 CGTAGATGAGGAAGATGGAGGTCTTCAAATCTGCC--------------------AATGGCTATCACTTCAATGTCATGAC
» PXR KO-4 CGTAGATGAGGAAGATGGAGGTCTTCAAATCTGCC--------------------AATGGCTATCACTTCAATGTCATGAC
   » WT-1  CGTAGATGAGGAAGATGGAGGTCTTCAAATCTGCCGTGTATGTGGGGACAAGGCCAATGGCTATCACTTCAATGTCATGAC
   » WT-2  CGTAGATGAGGAAGATGGAGGTCTTCAAATCTGCCGTGTATGTGGGGACAAGGCCAATGGCTATCACTTCAATGTCATGAC
   » WT-3  CGTAGATGAGGAAGATGGAGGTCTTCAAATCTGCCGTGTATGTGGGGACAAGGCCAATGGCTATCACTTCAATGTCATGAC
   » WT-4  CGTAGATGAGGAAGATGGAGGTCTTCAAATCTGCCGTGTATGTGGGGACAAGGCCAATGGCTATCACTTCAATGTCATGAC
  » RnPXR CGTAGATGAGGAAGATGGAGGTCTTCAAATCTGCCGTGTATGTGGGGACAAGGCCAATGGCTATCACTTCAATGTCATGAC
```

C

```
» CAR KO-1 ATGACAGCTACTCTAACACTAGAGACCATGACCAGT----------ATGGGCCAAGGAACTGTGTGGTGTGTGGAGGCCGA
» CAR KO-2 ATGACNGCTACTCTAACACTAGAGACCATGACCAGT----------ATGGGCCAAGGAACTGTGTGGTGTGTGGAGACCGA
» CAR KO-3 ATGACAGCTACTCTAACACTAGAGACCATGACCAGT----------ATGGGCCAAGGAACTGTGTGGTGTGTGGAGACCGA
» CAR KO-4 ATGACAGCTACTCTAACACTAGAGACCATGACCAGT----------ATGGGCCAAGGAACTGTGTGGTGTGTGGAGACCGA
   » WT-1  ATGACNGCTACTCTAACACTAGAGACCATGACCAGTGAAGAAGAGTATGGGCCAAGGAACTGTGTGGTGTGTGGAGACCGA
   » WT-2  ATGACAGCTACTCTAACACTAGAGACCATGACCAGTGAAGAAGAGTATGGGCCAAGGAACTGTGTGGTGTGTGGAGACCGA
   » WT-3  ATGACAGCTACTCTAACACTAGAGACCATGACCAGTGAAGAAGAGTATGGGCCAAGGAACTGTGTGGTGTGTGGAGACCGA
   » WT-4  ATGACAGCTACTCTAACACTAGAGACCATGNNNAGTGAAGAAGAGTATGGGCCAAGGAACTGTGTGGTGTGTGGAGACCGA
  » RnCAR ATGACAGCTACTCTAACACTAGAGACCATGACCAGTGAAGAAGAGTATGGGCCAAGGAACTGTGTGGTGTGTGGAGACCGA
```

Supplemental Figure 3. PXR and CAR mRNA Sequences from WT and PXR$^{-/-}$ and CAR$^{-/-}$ rats. A. cDNAs were generated via RT-PCR using specific oligonucleotides for the rat PXR and CAR cDNAs from liver RNA isolated from WT, PXR$^{-/-}$ and CAR$^{-/-}$ rats. The cDNAs were resolved by 2% E-gels (ThermoFisher, USA). B. cDNAs were cloned and sequenced with plasmid specific primers and WT and KO results aligned together using ContigExpress within Vector NTI Advance (Version 11.5.2; ThermoFisher, USA). Four representative sequences from WT and PXR$^{-/-}$ (B) and WT and CAR$^{-/-}$ (C) were aligned. Forty-eight individual sequencing results from each were used for the alignment. Forty-seven of the CAR$^{-/-}$ sequences were full length cDNA and one truncated, all that contained the deletion. Thirty-eight of the PXR$^{-/-}$ sequences were full length cDNA and six truncated, all that contained the deletion and four without readable sequence. All forty-eight WT sequences were in fact WT (ie. not deleted sequence). Dashed lines represents the respective deleted sequences for PXR$^{-/-}$ (B) and CAR$^{-/-}$ (C) cDNAs and the bottom sequence in each alignment is the rat cDNA sequence from NCBI for each gene.

Supplemental Figure 4.

A

MASMTGGQQMGRGSMRPEERWNHVGLVQREEADSVLEEPINVDEEDGGLQICRVCGDKANGYHFNVMTCEGCKGFFRRAMKRNVRLRC
PFRKGTCEITRKTRRQCQACRLRKCLESGMKKEMIMSDAAVEQRRALIKRKKREKIEAPPPGGQGLTEEQQLEHHHHHH

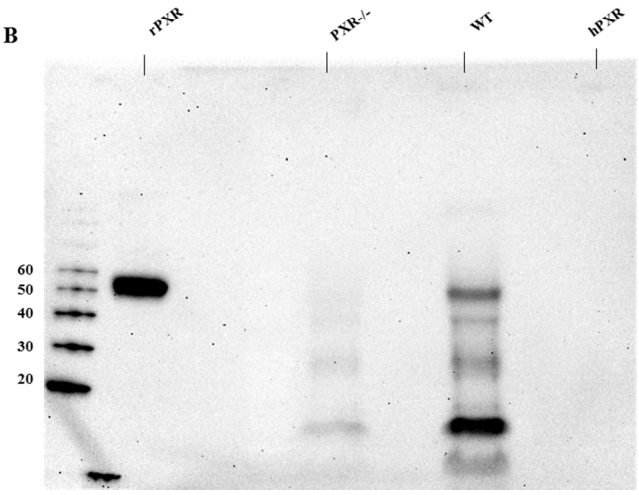

Supplemental Figure 4. Validation of anti-PXR antibody. (A) The amino acid sequence of the recombinant protein used for raising a PXR antibody. Rat PXR specific sequence is underlined. Arrow indicated the start of the deletion in PXR knockout rats. (B) Western blot analysis using the PXR antibody. Recombinant rat PXR (rPXR) is recognized and recombinant human PXR (hPXR) protein is not.

Supplemental Figure 5.

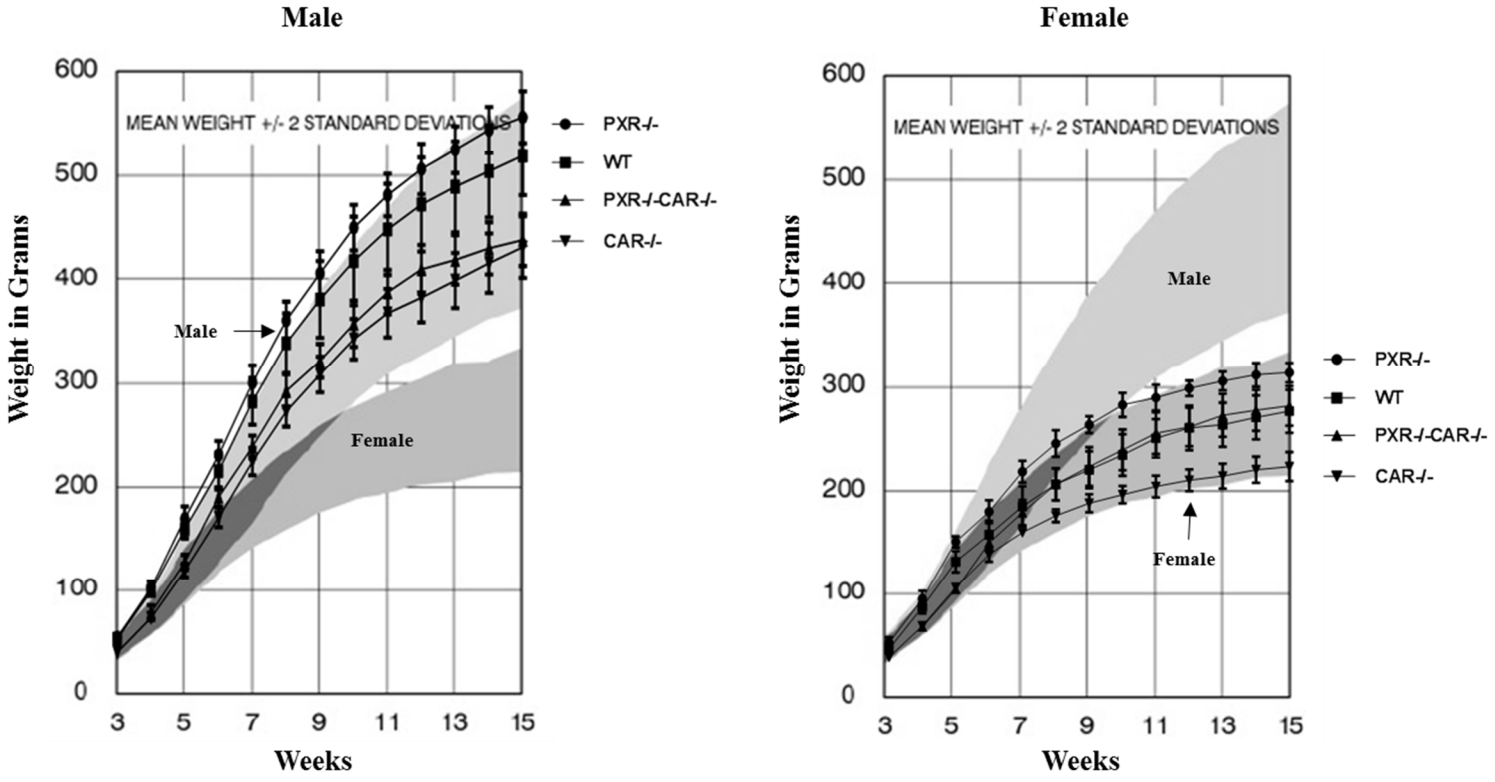

Supplemental Figure 5. Male and Female Rat Weights Compared to Charles River Laboratories Weight Data.

Our weight curves from Figure 2 superimposed on weight curves available for Sprague Dawley rats at Charles River Laboratories webpage (http://www.criver.com/products-services/basic-research/find-a-model/cd-igs-rat). As stated on CRL's graphs, the shaded areas represent mean weight +/- 2 standard deviations.

Supplemental Figure 6.

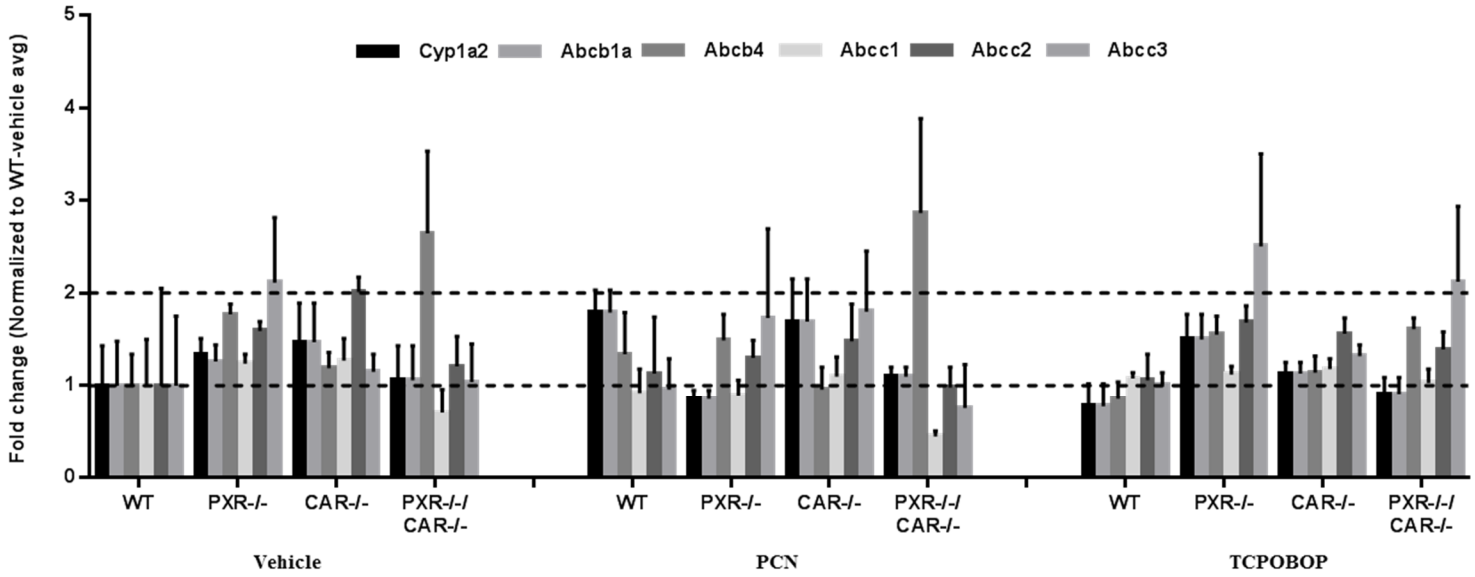

Supplemental Figure 6. Fold Change in Cyp1a2 and Drug Transporter Genes in Untreated and Treated Rats. Expression levels for Cyp1a2 and drug transporters Abcb1a, Abcb4, Abcc1, Abcc2, Abcc3 in vehicle (*left cluster*), PCN (*middle cluster*) and TCPOBOP (*right cluster*) treated rats that were normalized to WT vehicle treated rats to calculate fold changes. Fold change calculated by dividing each $2^{-\Delta CT}$ replicate (biologic) by the average WT vehicle $2^{-\Delta CT}$. Error bars are calculated standard deviation between the biological replicates. Dashed line represent normalized WT vehicle average value of 1. A second dash line of a value of 2 added to represent the range of no significant change in gene expression.

Supplemental Table 1. RT2 Custom Array CAPR11281 gene list

Gene Symbol	Alias	Refseq #	Official Full Name	RT2 Catalog Number
Nr1i3	CAR/MGC108525	NM_022941	Nuclear receptor subfamily 1, group I, member 3	PPR50285
Ahr	-	NM_013149	Aryl hydrocarbon receptor	PPR52899
Nr1h4	Fxr/MGC94878	NM_021745	Nuclear receptor subfamily 1, group H, member 4	PPR49558
Nr1i2	MGC108643/PXR	NM_052980	Nuclear receptor subfamily 1, group I, member 2	PPR50260
Rxra	-	NM_012805	Retinoid X receptor alpha	PPR56668
Rxrb	RXR-beta	NM_206849	Retinoid X receptor beta	PPR50385
Nr1h3	LXRalpha	NM_031627	Nuclear receptor subfamily 1, group H, member 3	PPR45298
Nr0b2	Shp	NM_057133	Nuclear receptor subfamily 0, group B, member 2	PPR45011
Nr5a2	Ftf/Lrh-1	NM_021742	Nuclear receptor subfamily 5, group A, member 2	PPR49556
Cyp2d4	Cyp2d18/Cyp2d22/Cyp2d4v1/Cyp2d4v2/Cyp2d6	NM_138515	Cytochrome P450, family 2, subfamily d, polypeptide 4	PPR48063
Cyp1a1	AHH/AHRR/CP11/CYP1/Cyp45c/Cypc45c/P-450MC/P1-450/P450-C/P450DX	NM_012540	Cytochrome P450, family 1, subfamily a, polypeptide 1	PPR57580
Cyp1a2	CYPD45/P-450d/RATCYPD45	NM_012541	Cytochrome P450, family 1, subfamily a, polypeptide 2	PPR43442
Cyp26a1	Cyp26	NM_130408	Cytochrome P450, family 26, subfamily A, polypeptide 1	PPR52263
Cyp26b1	-	NM_181087	Cytochrome P450, family 26, subfamily b, polypeptide 1	PPR46923
Cyp2b2	CYPIIB2/Cype	NM_001198676	Cytochrome P450, family 2, subfamily b, polypeptide 2	PPR63384
Cyp2c23	-	NM_031839	Cytochrome P450, family 2, subfamily c, polypeptide 23	PPR42691
Cyp2e1	Cyp2e	NM_031543	Cytochrome P450, family 2, subfamily e, polypeptide 1	PPR42474
Cyp3a23/3a1	CYP/CYP3A23/Cyp3a1/Cyp3a3/MGC108757/RL33/cDEX	NM_013105	Cytochrome P450, family 3, subfamily a, polypeptide 23/polypeptide 1	PPR52864
Cyp3a18	-	NM_145782	Cytochrome P450, family 3, subfamily a, polypeptide 18	PPR48486
Cyp3a2	Cyp3a11/MGC108545	NM_153312	Cytochrome P450, family 3, subfamily a, polypeptide 2	PPR48974
Cyp3a9	Cyp3a13/MGC93139/P450olf3	NM_147206	Cytochrome P450, family 3, subfamily a, polypeptide 9	PPR44879
Cyp4a1	Cyp4a10/Cyp4a22	NM_175837	Cytochrome P450, family 4, subfamily a, polypeptide 1	PPR53075
Cyp4a3	CYPIVA3/Cyp4a14	NM_175760	Cytochrome P450, family 4, subfamily a, polypeptide 3	PPR48625
Cyp7a1	CHAP/CYP7/CYP7S1	NM_012942	Cytochrome P450, family 7, subfamily a, polypeptide 1	PPR45025
Cyp2c11	CYP2CII/Cyp2c	NM_019184	Cytochrome P450, subfamily 2, polypeptide 11	PPR45096
Cyp2d2	Cyp2d26	NM_012730	Cytochrome P450, family 2, subfamily d, polypeptide 2	PPR52894
Cyp2c7	Cyp2c39/MGC156667	NM_017158	Cytochrome P450, family 2, subfamily c, polypeptide 7	PPR42439
Slco1a6	Oatp5/Slc21a13	NM_130736	Solute carrier organic anion transporter family, member 1a6	PPR61715
Slc22a6	MGC124962/Oat1/Orctl1/Paht/Roat1	NM_017224	Solute carrier family 22 (organic anion transporter), member 6	PPR52691
Abcg2	BCRP1	NM_181381	ATP-binding cassette, subfamily G (WHITE), member 2	PPR45780
Apoa5	MGC108612	NM_080576	Apolipoprotein A-V	PPR50286
Ppara	PPAR	NM_013196	Peroxisome proliferator activated receptor alpha	PPR44459
Pparg	-	NM_013124	Peroxisome proliferator-activated receptor gamma	PPR47599
Hnf4a	Hnf4/Hnf4alpha	NM_022180	Hepatocyte nuclear factor 4, alpha	PPR49773
Abcb1a	Abcb1/Mdr1a	NM_133401	ATP-binding cassette, sub-family B (MDR/TAP), member 1A	PPR56559
Abcb1b	Abcb1/Mdr1/Pgy1	NM_012623	ATP-binding cassette, subfamily B (MDR/TAP), member 1B	PPR52377
Abcb4	Mdr2/Pgy3	NM_012690	ATP-binding cassette, subfamily B (MDR/TAP), member 4	PPR57574
Abcc1	Abcc1a/Avcc1a/Mrp/Mrp1	NM_022281	ATP-binding cassette, subfamily C (CFTR/MRP), member 1	PPR44884
Abcc2	Cmoat/Mrp2	NM_012833	ATP-binding cassette, subfamily C (CFTR/MRP), member 2	PPR44758
Abcc3	Mlp2/Mrp3	NM_080581	ATP-binding cassette, subfamily C (CFTR/MRP), member 3	PPR52711
Rplp1	MGC72935	NM_001007604	Ribosomal protein, large, P1	PPR42363
Hprt1	Hgprtase/Hprt/MGC112554	NM_012583	Hypoxanthine phosphoribosyltransferase 1	PPR42247
Rpl13a	-	NM_173340	Ribosomal protein L13A	PPR53027
Ldha	Ldh1	NM_017025	Lactate dehydrogenase A	PPR56603
Actb	Actx	NM_031144	Actin, beta	PPR06570
RGDC	RGDC	U26919	Rat Genomic DNA Contamination	PPR63338
RTC	RTC	SA_00104	Reverse Transcription Control	PPX63340
PPC	PPC	SA_00103	Positive PCR Control	PPX63339

Supplemental Table 2. Taqman Assays

Gene Symbol	Alias	Refseq #	Official Full Name	Taqman Assay ID	Dye
Slco1a1	Oatp1	NM_017111.1	solute carrier organic anion transporter family, member 1a1	Rn00755148_m1	FAM
Slco1a2	Oatp2	NM_131906.1	solute carrier organic anion transporter family, member 1A2	Rn00756233_m1	FAM
Slc47a1	Mate1	NM_001014118.2	solute carrier family 47 (multidrug and toxin extrusion), member 1	Rn01460731_m1	FAM
Slc10a1	Ntcp	NM_017047.1	solute carrier family 10 (sodium/bile acid cotransporter), member 1	Rn00566894_m1	FAM
Ugt1a6		NM_001039691.2	UDP glucuronosyltransferase 1 family, polypeptide A6	Rn00756113mH	FAM
Ugt2b1	-	NM_173295.1	UDP glucuronosyltransferase 2 family, polypeptide B1	Rn00756519_m1	FAM
Ugt2b7	-	NM_173323.1	UDP glucuronosyltransferase 2 family, polypeptide B	Rn00821927_g1	FAM
Sult2a2	-	NM_001025131.1	sulfotransferase family 2A, dehydroepiandrosterone (DHEA)-preferring, member 2	Rn02586796_g1	FAM
Gstm4	-	NM_001024304.1	glutathione S-transferase mu 4	Rn01523449_g1	FAM
Ephx1	-	NM_001034090.3	epoxide hydrolase 1, microsomal (xenobiotic)	Rn00563349_m1	FAM
Reference genes					
ActB	-	NM_031144.3	actin, beta	Rn00667869_m1	VIC
Hprt1	Hprt	NM_012583.2	hypoxanthine phosphoribosyltransferase 1	Rn01527840_m1	VIC
Gapdh	Gapd	NM_017008.4	glyceraldehyde-3-phosphate dehydrogenase	Rn01775763_g1	VIC

Supplemental Table 3. Gene expression in Vehicle Treated Rats Compared to WT

P450 Gene	PXR$^{-/-}$	CAR$^{-/-}$	PXR$^{-/-}$/CAR$^{-/-}$
Cyp2b2	9.61*	0.11	7.15*
	(+/- 2.86)	(+/- 0.05)	(+/- 2.66)
Cyp3a23/3a1	4.54*	1.22	6.15*
	(+/- 0.44)	(+/- 0.15)	(+/- 3.02)
Cyp3a18	3.89*	1.07	5.43*
	(+/- 0.06)	(+/- 0.09)	(+/- 2.84)
Cyp3a2	3.59*	0.69	14.58*
	(+/- 0.23)	(+/- 0.06)	(+/- 13.95)
Cyp3a9	0.61	3.60*	7.35*
	(+/- 0.18)	(+/- 1.29)	(+/- 6.73)
Slco1a2	1.04	1.12	0.87
	(+/-0.41)	(+/- 0.49)	(+/- 0.36)
Slco1a1	1.28	1.74	0.92
	(+/- 0.55)	(+/- 0.50)	(+/- 0.29)
Slc10a1	1.45	1.22	0.89
	(+/- 0.58)	(+/- 0.53)	(+/- 0.36)
Ugt2b1	4.57*	0.49	4.14*
	(+/- 1.39)	(+/- 0.14)	(+/- 1.73)
Ugt1a6	0.66	0.85	0.52
	(+/- 0.26)	(+/- 0.37)	(+/- 0.21)
Sult2a2	1.48	1.07	2.01
	(+/- 0.41)	(+/- 0.30)	(+/- 0.84)
Ephx1	1.97	1.97	1.53
	(+/- 0.78)	(+/- 0.86)	(+/- 0.62)
Gstm4	1.19	1.09	0.91
	(+/- 0.47)	(+/- 0.48)	(+/- 0.37)

Values are relative to vehicle treated wild type rats, +/- standard deviation. Data was analyzed by one-way ANOVA followed by Tukey's multiple comparison test. * = significantly different from WT ($p<0.05$, Tukey's)